arXiv:cond-mat/0311494v1 [cond-mat.mes-hall] 20 Nov 2003

Tunable terahertz emission from difference-frequency in biased superlattices

Ren-Bao Liu[1] and Bang-Fen Zhu[1]

[1]*Center for Advanced Study, Tsinghua University, Beijing 100084, China*

The terahertz emission from difference-frequency in biased superlattices is calculated with the excitonic effect included. Owing to the doubly resonant condition and the excitonic enhancement, the typical susceptibility is larger than 10^{-5} m/V. The doubly resonant condition can always be realized by adjusting the bias voltage and the laser frequencies, thus the in-situ tunable emission is efficient in the range of 0.5–6 terahertz. Continuous wave operation with 1% quantum efficiency and μW output power is feasible while the signal absorption in undoped superlattices is negligible.

PACS numbers: 78.20.Bh, 42.65.An, 42.65.Yj, 73.21.Cd

Terahertz (THz) electromagnetic waves have potential applications in many fields, like medical diagnosis, environment monitoring, high-speed communication, astronomy spectroscopy, etc. [1]. Though intense tunable THz emission from free-electron lasers is available in laboratories [2], tunable tabletop THz sources are still desirable for practical applications. To obtain THz emission from small semiconductor devices, many schemes have been studied, such as coherent phonons [3], wave-packet oscillation in asymmetric quantum wells [4], heavy-light hole beatings [5], Bloch oscillations [6], and difference-frequency in doped quantum wells [7]. With state-of-the-art design of superlattices, a prototype of quantum-cascade THz lasers has been demonstrated recently [8]. Among these mechanisms for THz emission, the difference-frequency process is of special interest because of its in-situ tunability, intense output under phase-matching condition, and flexibility of operating at both continuous wave and pulse modes [9]. Furthermore, doubly resonant condition, in which both the input and output are near resonant with transitions in the system, can also be exploited to enhance the difference-frequency [7].

Doubly resonant difference-frequency in biased superlattices was also proposed for THz emission [10, 11]. Under doubly resonant condition, the Bloch oscillation is sustained and amplified by the effective THz potential resulting from the dipole interaction of excitons and the bichromatic input light, generating efficient THz radiation [10]. Several advantages of this method over other difference-frequency schemes can be expected: First, the applied electric field breaks the inversion symmetry of the system, leading to a large intraband dipole matrix element. Secondly, the doubly resonant condition can always be accomplished by adjusting the static electric field and tuning the input light. And thirdly, the problem of signal absorption can also be avoided in undoped superlattices.

Though it has been well-known that the exciton correlation plays an essential role in THz emission from Bloch oscillation in optically excited superlattices [12], its effect on difference-frequency in biased superlattices is still unclear. This question will be addressed in this Letter, and it will be shown that the excitonic effect can enhance the emission power by at least two orders of magnitude, which, however, is absent in, e.g., difference-frequency in doped quantum wells [7].

The second-order difference-frequency susceptibility is the key quantity determining the emission intensity. In principle, it can be evaluated from the textbook formula derived with the double-line Feynman diagrams [13]. Under the doubly resonant condition, the difference-frequency susceptibility [13]

$$\chi^{\rm diff}_{jj_1j_2}(\omega=\Omega_1-\Omega_2;\Omega_1,-\Omega_2)\approx\sum_{a,b}(V\epsilon_0)^{-1}\times\left[\frac{(d_{j_2})_{0b}(d_j)_{ba}(d_{j_1})_{a0}}{(\varepsilon_{ba}+i\hbar\gamma_1+\hbar\omega)(\varepsilon_{a0}-i\hbar\gamma_2-\hbar\Omega_1)}+\frac{(d_{j_2})_{0b}(d_j)_{ba}(d_{j_1})_{a0}}{(\varepsilon_{ab}-i\hbar\gamma_1-\hbar\omega)(\varepsilon_{b0}+i\hbar\gamma_2-\hbar\Omega_2)}\right], \quad (1)$$

where Ω_i is the frequency of the input light polarized at $\mathbf{e}_{j_i}$ direction, $\varepsilon_{\alpha\alpha'}$ (α, $\alpha'=a$, b, or 0) is the transition energy between the exciton states $|a\rangle$, $|b\rangle$, and the semiconductor ground state $|0\rangle$, $\mathbf{d}_{\alpha\alpha'}$ is the dipole matrix element, γ_2 and γ_1 are the interband and intraband dephasing rates, respectively, V is the volume of the sample, and ϵ_0 is the vacuum dielectric constant.

With the excitonic effect neglected, the susceptibility of biased superlattices can be analytically evaluated [11], and the result turns out comparable to that of doped quantum wells and larger by many orders of magnitude than that of bulk semiconductors [13, 14]. The Coulomb coupling, however, makes it a formidable task to calculate the susceptibility directly from Eq. (1), since all the excitonic eigen states should be obtained. To avoid such an exhausting work, we have developed a time-domain technique, in which the susceptibility is first transformed into the time domain, and the result numerically calculated is transformed back to the frequency domain by standard fast Fourier transformation.

By Fourier transformation of Eq. (1), the time-domain susceptibility of biased superlattices can be derived as

$$\chi^{\rm diff}_{zj_1j_2}(t;t_1,t_2)=\frac{1}{\omega+i\gamma_1}\frac{e}{4\epsilon_0\hbar^3}\int d\boldsymbol{\rho}\sum_{l,m}$$

$$m\lambda_m\psi^*_{j_2}(\boldsymbol{\rho},l-m,t-t_2)\psi_{j_1}(\boldsymbol{\rho},l,t-t_1)$$
$$\times\left[\theta(t-t_1)\theta(t_1-t_2)e^{-\gamma_1(t-t_1)-\gamma_2(t_1-t_2)}\right.$$
$$\left.+\theta(t-t_2)\theta(t_2-t_1)e^{-\gamma_1(t-t_2)-\gamma_2(t_2-t_1)}\right], \quad (2)$$

in which the exciton Green's function satisfies the motion equation in the tight-binding model

$$i\hbar\partial_t\psi_j(\boldsymbol{\rho},l,t)=\left[E_g-(2\mu)^{-1}\hbar^2\boldsymbol{\nabla}^2_{\boldsymbol{\rho}}\right]\psi_j(\boldsymbol{\rho},l,t)$$
$$+\sum_m\left(leFD\delta_{m,0}-\lambda_m/4\right)\psi_j(\boldsymbol{\rho},l+m,t)$$
$$+V(\boldsymbol{\rho},l)\psi_j(\boldsymbol{\rho},l,t)-\hbar(d_j)_{\rm cv}\delta(\boldsymbol{\rho})\delta_{l,0}\delta(t), \quad (3)$$

where λ_m is the tunnelling coefficient between quantum wells separated by $|m|$ barriers, $\boldsymbol{\rho}$ denotes the in-plane coordinates in real space, l is the index of the unit cell of the superlattice, E_g is the distance between the centers of the electron and hole minibands, μ is the reduced effective mass of the electron-hole pair, D is the superlattice period, F is the strength of the static field, and $V(\boldsymbol{\rho},l)$ is the Coulomb potential. In the derivation of Eq. (2), only the lowest electron and heavy-hole minibands are included, and the Coulomb potential, assumed slow-varying as compared to the superlattice potential, takes the form

$$V(\boldsymbol{\rho},l)=-e^2(4\pi\epsilon_0\epsilon)^{-1}\left(\rho^2+l^2D^2\right)^{-1/2}, \quad (4)$$

where ϵ is the dielectric constant of the material. It would not be difficult to include more complexity of realistic semiconductor systems, such as the valence-band-mixing and the Coulomb coupling between minibands, which, however, is expected to modify the results only in details.

The most important feature of Eq. (2) is that the susceptibility has the form of exciton-exciton correlation. Thus the difference-frequency susceptibility, as well as linear absorption spectra, can be evaluated by just integrating the motion equation for the exciton wavefunction [Eq. (3)], which can be done with the space-time difference method proposed by Glutsch *et al.* [15]. To check the numerical method, the susceptibility has been numerically calculated with the Coulomb potential artificially switched off and compared to the analytical result [11], the deviation is always less than one percent.

Now let us focus on the excitonic case. To be specific, here we consider a superlattice sample that has been well studied for Bloch oscillation [16], namely, a $GaAs/Al_{0.3}Ga_{0.7}As$ superlattice with 67 Å well width and 17 Å barrier width. A Kronig-Penney calculation shows that the lowest electron and hole minibands have almost perfect cosinusoid dispersions and the combined miniband width is about 41 meV, so $\lambda_m \approx \delta_{|m|,1}\times 41$ meV. With the miniband width larger than the emission threshold of optical phonons, the relaxation in this sample is very rapid, so the interband and intraband dephasing rates are chosen quite large values: $\gamma_1^{-1}=0.6$ ps and $\gamma_2^{-1}=0.3$ ps. The interband dipole matrix element

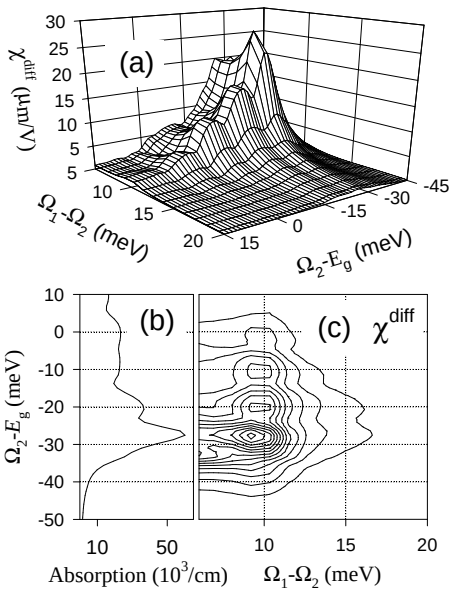

FIG. 1: (a) The 3D plot of the difference-frequency susceptibility of a biased superlattice vs. the output frequency and one of the input frequencies. (b) The linear absorption spectrum of the superlattice. (c) The contour plot of the difference-frequency susceptibility.

obtained from the $\mathbf{k}\cdot\mathbf{p}$ theory is $d_{\rm cv}\approx 6.5$ eÅ. Other parameters are such that the excitonic binding energy is 4.9 meV, the band gap $E_g=1.511$ eV, the static dielectric constant $\epsilon=12.9$, and the optical refractive index $n=3.26$.

The difference-frequency susceptibility has been calculated for various static field strength. A typical example is plotted in Fig. 1 for $F=11.9$ kV/cm (correspondingly, the frequency of the free-particle Bloch oscillation $\nu_{\rm BO}=2.44$ THz, or $h\nu_{\rm BO}\equiv eFD=10$ meV). The doubly resonant effect is evident in the peak features of the susceptibility spectrum. The Coulomb interaction renormalizes the interband transition energy and the Bloch oscillation frequency. More importantly, as compared to the free-particle result [see Fig. 2 (a)], the excitonic effect enhances the susceptibility by more than one order of magnitude. The excitonic enhancement results mainly from the enhancement of the oscillator strength at band edge (due to the Sommerfield factor). The Sommerfield factor also induces extra absorption at band edge, but considering the fact that the linear optical absorption is proportional to the second power of the interband dipole matrix element while the THz signal intensity is proportional to the fourth power, the net effect of Coulomb interaction is advantageous to the difference-frequency process.

To estimate the power of the THz emission, we assume perfect phase-matching for the optical mixing, which can be achieved just geometrically since the refractive index

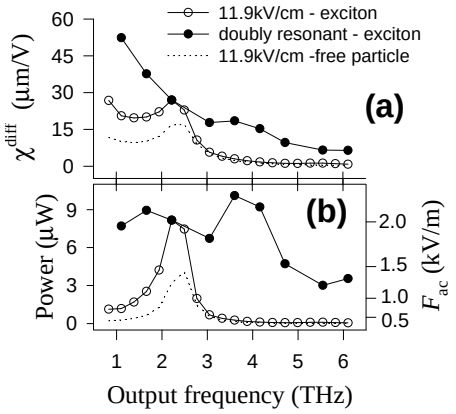

FIG. 2: (a) The difference-frequency susceptibility and (b) the power of the THz emission as functions of the frequency difference. In (b), the THz field strength $F_{\rm ac}$ is also indicated. The solid lines with open circles represent excitonic results at fixed field strength $F = 11.9$ kV/cm and optimized input light frequency, while the solid lines with close circles correspond to excitonic results with both the static field and the optical frequencies adjusted to maximize the emission power. The dotted lines plot the free-particle results at fixed electric field (11.9 kV/cm) and optimized optical frequencies. For visibility, the susceptibility and emission power in the free-particle case are magnified by a factor of 10 and 100, respectively.

at THz waveband is larger than that in optical frequency. The spot size of the laser beams with appropriate incident angles is taken as $l_x \times l_y$. Thus the power of the THz signal propagating along the in-plane x-direction is roughly

$$P_{\rm THz} \approx \omega^2 \left|\chi^{\rm diff}\right|^2 ND \left(8 l_y c^3 \epsilon_0 \epsilon^{1/2} n^2\right)^{-1} P_1 P_2, \quad (5)$$

where P_1 and P_2 are the power of the two input laser beams, N is the number of the superlattice periods, and c is the vacuum light velocity. To be specific, we use following realistic parameters: $N = 50$, $P_1 = P_2 = 0.1$ W, and $l_y = 1$ mm.

In Fig. 2, the difference susceptibility and the THz emission power are plotted against the output frequency both for a fixed static field and for doubly resonant condition. For comparison, the results without Coulomb interaction are also shown for the fixed field strength. The excitonic effect enhances the emission power by more than two orders of magnitude. Under doubly resonant condition, the power of THz emission is several μW, and the THz electric field strength is larger than 1 kV/m. The efficiency of converting near infrared photons to THz photons is around 1%. Because the doubly resonant condition can always be realized by simultaneously adjusting the bias voltage and laser frequencies, the THz emission power is not sensitive to the frequency difference in the range of 0.5–6 THz, which, under fixed static field, would otherwise decreases rapidly as the frequency difference goes away from the Bloch oscillation frequency.

Negligible absorption of THz signals is another advantage of using biased superlattices for difference-frequency over other doubly-resonant schemes, such as that in doped quantum wells. For parameters in the example above, the optically excited carrier density, with continuous wave operation mode and 1 ns^{-1} recombination rate assumed, is of the order of 10^9 cm^{-2} per quantum well, and there is basically no free carriers outside the laser spot, so the THz signal can propagate without significant absorption by electrons. Neither is the signal absorption by optical phonons crucial in the frequency range considered.

In conclusion, the in-situ tunable THz emission from difference-frequency in biased superlattices is quite efficient owing to the tunable doubly-resonant condition, the excitonic enhancement, and negligible absorption of signals.

The authors are grateful to J. Wu for providing computer facilities. This work was supported by the National Science Foundation of China.

[1] B. Ferguson and X.-C. Zhang, Nature Materials **1**, 26 (2002).
[2] G. Ramian, Nucl. Instrum. Methods Phys. Res. A **318**, 225 (1992).
[3] W. Kütt, G. C. Cho, T. Pfeiffer, and H. Kurz, Semicond. Sci. Technol. **7**, B77 (1992).
[4] H. G. Roskos, M. C. Nuss, J. Shah, K. Leo, A .B. Miller, A. M. Fox, S. Schmitt-Rink, and K. Köhler, Phys. Rev. Lett. **68**, 2216 (1992).
[5] P. C. M. Planken, M. C. Nuss, I. Brener, K. W. Goossen, M. S. C. Luo, S. L. Chuang, and L. Pfeiffer, Phys. Rev. Lett. **69**, 3800 (1992).
[6] H. G. Roskos, Adv. Solid State Phys. **34**, 297 (1994),
[7] C. Sirtori, F. Capasso, J. Faist, L. N. Pfeiffer, and K. W. West, Appl. Phys. Lett. **65**, 445 (1994).
[8] R. Köhler, A. Tredicucci, F. Beltram, H. E. Beere, E. H. Linfield, A. G. Davies, D. A. Ritchle, R. C. Iotti, and F. Rossi, Nature (London) **417**, 156 (2002).
[9] J. Y. Sohn, Y. H. Ahn, D. J. Park, E. Oh, and D. S. Kim, Appl. Phys. Lett. **81**, 13 (2002).
[10] R. B. Liu and B. F. Zhu, Europhys. Lett. **50**, 526 (2000).
[11] A. V. Korovin, F. T. Vasko, and V. V. Mitin, Phys. Rev. B **62**, 8192 (2000).
[12] V. M. Axt, G. Bartels, and A. Stahl, Phys. Rev. Lett. **76**, 2543 (1996).
[13] Y. R. Shen, *The Principles of Nonlinear Optics* (John Wiley & Sons, New York, 1984).
[14] Y. R. Shen, Progr. Quant. Electro. **4**, 207 (1976).
[15] S. Glutsch, D. S. Chemla, and F. Bechstedt, Phys. Rev. B **54**, 11592 (1996).
[16] P. Leisching, P. Haring Bolivar, W.Beck, Y. Dhaibi, F. Brüggemann, R. Schwedler, K. Kurz, K. Leo, and K. Köhler Phys. Rev. B **50**, 14 389 (1994).